

Methane steam reforming at low temperature
over Ni-MgO-Al₂O₃ catalysts:
activity and resistance to coking

Monika Pańczyk^a, Andrzej Denis^a, Kazimierz Stołecki^b
and Tadeusz Borowiecki^{a,*}

^a *Faculty of Chemistry, Maria Curie-Skłodowska University,
20-031 Lublin, Poland*

^b *New Chemical Synthesis Institute, 24-100 Puławy, Poland*
**e-mail: tadeusz.borowiecki@umcs.lublin.pl*

The role of MgO as a factor improving the resistance to coking of the alumina supported nickel catalysts in the steam reforming of hydrocarbons is discussed. A series of catalysts containing variable amounts of MgO, NiO and a constant amount of Al₂O₃ was prepared by the co-precipitation method. It was found that the specific activity of the catalysts exhibits a broad but not deep minimum for the MgO contents from 8.5 to 27.3 wt.%. At the same time these catalysts reveal a high resistance to coking either in the reaction with methane or with *n*-butane. The most promising composition, in terms of the activity and simultaneous resistance to the coke formation, was found to be 27.3 wt.% of MgO and 39.0 wt.% of NiO. The analysis of various factors controlling the activity and resistance to coking leads to the conclusion that MgO reduces the catalysts acidity what, in consequence, reduces the rate of coke formation during the reforming reactions. Furthermore, The resistance to coking correlates well with the mean size of nickel crystallites, the same is observed for the specific catalyst activity.

1. INTRODUCTION

The problem of the carbon deposits formation on catalysts surfaces in processes involving the synthesis gas or hydrogen production (steam reforming of higher hydrocarbons, steam reforming of natural gas at low steam to methane ratio, or carbon dioxide reforming of hydrocarbons) has been attracting a considerable interest in the field of nickel catalysts with an improved resistance to coking.

One of the methods of improving the catalyst quality is a modification of the carrier composition (typically α -Al₂O₃), leading to the systems exhibiting enhanced resistance either to coking or sintering [1–3]. The Ni/Al₂O₃ catalysts are often modified by the incorporation of MgO. It may be introduced into a catalyst by utilizing magnesium aluminum spinel as a carrier or by doping the Al₂O₃ structure with MgO using various preparation techniques and MgO contents.

The composite catalysts comprising NiO, MgO and Al₂O₃ are interesting though, at the same time, they are difficult for systematic studies [4–7]. A complex influence of MgO on the catalyst properties is a result of the formation of NiO–MgO solid solutions [8, 9], changes of the NiO reduction degree and nickel dispersion [7, 10], changes of the surface acidity [11] as well as an interaction of the catalyst with components of the reaction mixture [12].

Recently, a highly resistant to coking of NiO–MgO catalysts, designed for carbon dioxide reforming of methane, have taken center stage [3, 13, 14]. However, these catalysts have got limited development perspectives in the case of the steam reforming of methane [12, 15].

Furthermore, there has been also a considerable interest in the natural gas steam reforming carried out at low temperatures and, thus, providing significant financial and environmental advantages [16, 17].

The aim of this work is a comprehensive study of the influence of the catalysts composition (NiO and MgO content) on the properties of co-precipitated NiO–MgO–Al₂O₃ systems. The results obtained should help to design a highly active, resistant to deactivation (coking, sintering) and, at the same time, cheap catalyst for the steam reforming of methane. These catalysts might be used in e.g. autothermal reformers (ATR) generating a various purpose synthesis gas with a variable H₂:CO ratio. Previous studies revealed that thermally stable NiO–Al₂O₃ catalytic systems could be obtained for at least 30 wt.% content of Al₂O₃ in the catalysts. A subsequent modification of the initial catalyst composition was accomplished by altering the proportion of the other components

(NiO and MgO) leading finally to the composite systems with various proportions of NiO and MgO but the constant amount of Al₂O₃. The choice of that approach has been dictated by a well-known strong influence of MgO on the resistance to coking of the nickel catalysts [18–21].

2 MATERIALS AND METHODS

2.1 Catalyst preparation and characterization

The Ni-MgO-Al₂O₃ catalysts were prepared by the co-precipitation method from the solutions of corresponding nitrates with sodium carbonate. The precipitates were filtered, washed with distilled water, dried and calcined for 4 h at 400°C. The content of Al₂O₃ in the obtained catalysts was about 30 wt.%, while the amount of Ni expressed in terms of NiO varied from 70 to 20 wt.% (Table 1). The composition of the catalysts was determined by the X-ray fluorescence method (XRF) using a Philips X-Unique II spectrometer. The total surface area (S_{BET}) of the catalysts after reduction performed at 800°C for 3 h was determined by the argon adsorption method at the LN₂-temperature (LN₂ – liquid nitrogen) in the static-volumetric apparatus. The active nickel surface area (S_A) after reduction was determined in the same apparatus by the hydrogen chemisorption method at 20°C under 100 mmHg pressure, assuming the chemisorption stoichiometry H:Ni = 1:1, and that the surface area occupied by a single hydrogen atom was 0.065 nm² [22]. The mean size of nickel crystallites was determined using the following relationship:

$$d_H = \frac{5 \cdot 10^3}{\gamma_{\text{Ni}} S_H} \text{ (nm)} \quad (1)$$

where: γ_{Ni} – nickel density, S_H – surface area of 1 g of the reduced nickel.

X-ray diffraction studies of the reduced samples after passivation in technical grade nitrogen were carried out with a HZG-4 diffractometer using monochromatic Cu-K α radiation. The mean size of nickel crystallites (after reduction) was calculated from the width of X-ray diffraction lines fitting the Scherrer equation [23]. The phase composition identification of samples was carried out using XRAYAN software in the 2 Θ range from 20 to 90°.

2.2 *Studies of the catalytic activity*

The measurements were carried out in a Zielinski-type reactor [24] under ambient pressure and in the kinetic regime using the samples after reduction for 3 h at 800°C in the hydrogen stream. The reactor was supplied by the stream of reagents composed by mixing methane (diluted in argon) with hydrogen (4 vol. %) using the mass flow controllers. The gas stream was saturated with water vapor in the saturator. The composition of the post-reaction mixture was monitored at the reactor outlet. The contents of CO, CO₂ and CH₄ were analyzed using a Philips PU-4500 gas chromatograph equipped with a CO and CO₂ methanizer and a FID (Flame Ionization Detector) detector with an accuracy of 10 ppm vol. The activity measurements were carried out at three temperatures, i.e. 450, 500 and 550°C using the reaction mixtures containing not more than 1.5 vol.% of methane and for H₂O:CH₄ reagents ratio in the range 1.4–6:1.

2.3 *Studies of the catalysts coking*

The measurements of the resistance to coking were carried out according to the following approaches: (i) the temperature-programmed surface reaction (TPSR) aimed at determining the temperature of the coking initiation in the steam reforming of methane; and (ii) the gravimetric method, in a plug flow quartz reactor, aimed at determining the rate of coking in the steam reforming of *n*-butane.

2.3.1. Temperature-programmed surface reaction (TPSR)

The TPSR method is commonly applied to study the resistance to coking of nickel catalysts, revealing significant differences in the texture and chemical composition [25, 26]. The measurements were carried out using a Cahn TG121 microbalance in a plug flow quartz microreactor for various reaction mixtures. The measurements of the coking initiation temperatures were performed for the catalysts grain fraction in the range 0.3–0.5 mm.

The studies of the coking initiation temperature in the steam reforming of methane were carried out using the reaction mixtures CH₄ + H₂O + H₂ + He, under the constant flow rate of 70 cm³/min, constant partial pressure of methane $p_{CH_4}/p_0 = 0.34$ and the variable water vapor or hydrogen amounts in the ranges corresponding to the molar ratios H₂O:CH₄ = 0–0.8 and H₂:CH₄ = 0.33–1.0. After reduction the reactor was cooled down to 400°C and the reducing mixture

(He + 10% H₂) was replaced by the reaction mixture. It was followed by 15 min of the stabilization period and the dynamics of the process was then recorded under the constant heating rate 5°C/min up to 800°C.

2.3.2. Isothermal gravimetric studies of coking

This method allows the estimation of the carbon deposits amount formed as a change of the sample weight. Normally, the sample is placed in a porous container, hanging on a balance beam, which, in turn, is placed in a working reactor.

The studies of the coking process in the steam reforming reaction of *n*-butane were carried out at the temperature of 500°C, under the constant partial pressure of *n*-butane $p_{C_4H_{10}}/p_0 = 0.06$ and at two steam to *n*-butane ratios, i.e. H₂O:C₄H₁₀ = 0.5 and 1.5. Various reagents ratios in the mixture were obtained by changing the partial pressure of the water vapor. The total volumetric flow rate of the mixture (500 cm³/min) was kept constant by adding nitrogen which, as we assume, does not affect the reaction mechanism.

2.4 Morphology of carbon deposits

The morphology of carbon deposits was studied using high-resolution transmission electron microscopy (HTREM). The coked catalyst samples after being crushed in agate mortar were treated with 99.8% ethanol (POCH Gliwice, Poland) to form suspension and then it was ultrasonically homogenized for 20s. Afterwards, it was placed on copper mesh (200 lines/inch – 200 mesh) covered with lacely formvar stabilized carbon (Ted Pella) and left on the filter paper until ethanol evaporated. Titan G2 60-300 kV (FEI Company) electron microscope was used to visualize the catalyst samples. It was equipped with FEG – Field Emission Gun, monochromator, lens system, image corrector (C_s-corrector), and HAADF (high-angle annular dark-field) detector. Microscope measurements were carried out at an accelerating electron beam voltage of 300 kV.

2.5 Carbon deposits gasification

In the experimental setup described in section 2.3.2. the catalysts were coked in the steam reforming of *n*-butane at the temperature of 500°C (isothermal studies) using the reagents ratio H₂O:C = 0.5. After obtaining ~25 % of coke, in reference to the initial catalyst weight, the

gasification in the stream of the deoxidized and dried hydrogen was performed.

The temperature-programmed oxidations (TPO) were carried out using an AMI-1 (Altamira Instruments Inc.) setup equipped with a HAL 201 RC (Hiden Analytical Ltd) mass spectrometer, using a plug flow quartz reactor with an internal diameter of 10 mm. The samples of ca. 0.05 g were heated with the heating rate of 10°C/min in the mixture 5%O₂/He (Praxair) using the flow rate 30 cm³/min. The intensities of signals corresponding to the ions with $m/z = 2, 16, 18, 28, 30, 32, 44$ were recorded continuously.

3. RESULTS

3.1. Temperature-programmed reduction

The temperature-programmed reduction (TPR) profiles of the samples studied have already been published [27]. The increasing of MgO content diminishes the reducibility of the catalysts. It is related to the formation of the NiO–MgO solid solutions [8, 28] as well as NiO–Al₂O₃ compounds [17, 29]. The shape of the TPR curves shows, that the reduction process occurs in two temperature regimes (Table 1).

Table 1. The hydrogen uptake and reduction degree of the NiO–MgO–Al₂O₃ catalysts.

Catalyst	Weight ratio MgO/NiO	Hydrogen uptake				T_{max} [°C]	NiO reduction degree [%]
		[mmol/g _{cat}]	[mmol/g _{NiO}]				
			up to 400°C	from 400 to 900°C	total		
B0	0.00	7.48	0.28	10.48	10.7	703	81
B1	0.14	6.79	0.93	10.07	11.0	749	82
B2	0.32	5.51	0.71	9.69	10.4	772	78
B3	0.47	4.55	0.47	9.43	9.9	798	74
B4	0.70	3.56	0.43	8.67	9.1	837	68
B5	1.5	1.95	0.47	6.86	7.3	864	55

Small hydrogen consumption are observed in the range 200–400°C but the most essential is the range 400–900°C. In both ranges, the reduction process depends on the catalyst composition. The maximum of the main peak shifts from ~700°C (B0) to ~860°C (B5). The increasing amounts of MgO hinder the reduction process, as evidenced by the decreasing NiO reduction degree for higher and higher amounts of MgO in the catalyst.

3.2. Physicochemical properties of the catalysts

The physicochemical properties of the catalysts under study are collected in Table 2.

Table 2. The physicochemical properties of the studied Ni-MgO-Al₂O₃ catalysts

Catalyst	Composition (wt.%)		Weight ratio MgO/NiO	Surface area (m ² /g _{cat.})		Mean nickel crystallite size (nm)	
	NiO	MgO		total	active	d _H ^a	d _x ^b
B0	69.5	0.0	0.00	69.1	29.3	9.7	7.7
B1	61.7	8.5	0.14	79.1	32.4	6.9	4.9
B2	53.0	17.2	0.32	88.2	30.6	6.3	4.9
B3	46.0	21.4	0.47	88.8	23.4	6.4	4.8
B4	39.0	27.3	0.70	92.1	17.7	6.4	3.7
B5	26.6	38.9	1.50	95.4	8.4	5.2	5.9

a – determined from hydrogen chemisorption data.

b – determined from X-ray diffraction data.

Figure 1 shows, how the MgO content affects some of these crucial parameters. The total surface area S_{BET} gradually increases with the increasing MgO content. The values of the active surface area initially increase upon incorporation of small amounts of MgO, and then decrease as the MgO/NiO ratio increases.

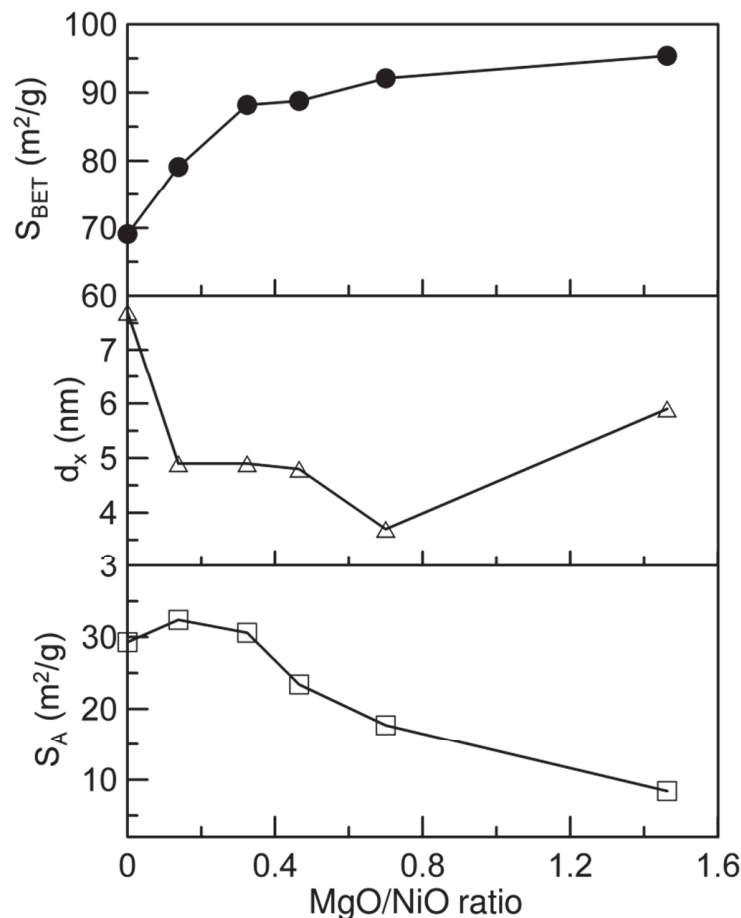


Fig. 1. Changes of the total S_{BET} and active S_A surface areas and the mean size of nickel crystallites d_x as a function of the MgO/NiO ratio after reduction at 800°C.

Furthermore, the data reveal a decreasing trend of the mean size of nickel crystallites with the increasing MgO content. This phenomenon is most probably related to the formation of the NiO–MgO solid solutions in the catalysts [2, 8, 9, 30, 31].

X-ray powder diffraction patterns of the samples after reduction have already been published [27]. The hydrotalcite-like phases are not observed after reduction. The XRD patterns evidence the presence of metallic nickel crystallites (#PDF 04-850) with reflection lines at 2θ angle 44.5° and 51.9° . The additional small peaks (e.g. at $\sim 37^\circ$ or 62°) are observed for MgO containing samples. The nickel crystallites size slightly decreases with the increasing Mg/Ni ratio in the samples (Table 2).

3.3. Activity measurements in the steam reforming of methane

The activity measurements were carried out at three temperatures: 450, 500 and 550°C, as a function of the reagents H₂O:CH₄ ratio. Figure 2 shows, as an illustration, the activity of the catalysts at the temperature 550°C, with the reagents mixture containing 4% of H₂.

The catalysts activity increases with the increasing H₂O:CH₄ ratio. The highest activity is exhibited by the reference B0 catalyst containing the highest amount of nickel (without MgO). The decreasing activity of the other catalysts is due to the decreasing amount of nickel and increasing MgO:NiO ratio. It is worth noting that the most noticeable change of the activity occurs after incorporation of 8.5% of MgO. Further increase of MgO, up to 38.9%, leads to a gradual though not rapid decrease of the activity.

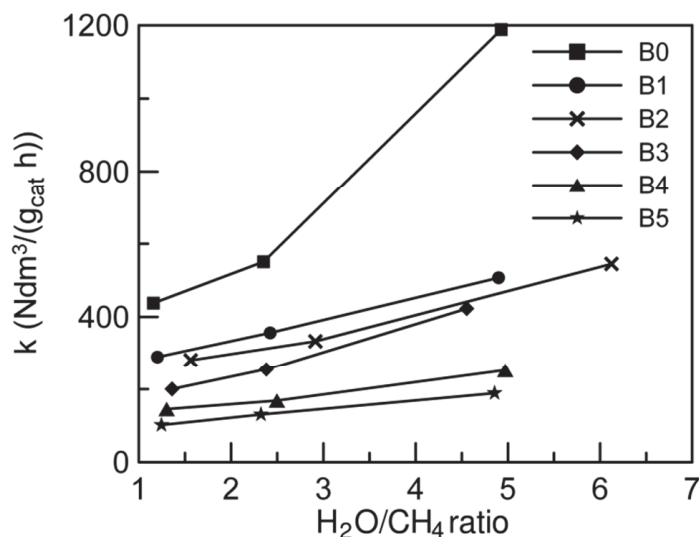


Fig. 2. The rate constant as a function of the reagents H₂O:CH₄ ratio at the temperature 550°C and at the constant amount (4%) of H₂ in the reaction mixture.

Figure 3 shows how the MgO/NiO ratio affects the rate constants, determined for the H₂O:CH₄ = 2 ratio and recalculated to 1 g of the catalysts, 1 m² of the active nickel area and 1 g of NiO in the catalyst, respectively.

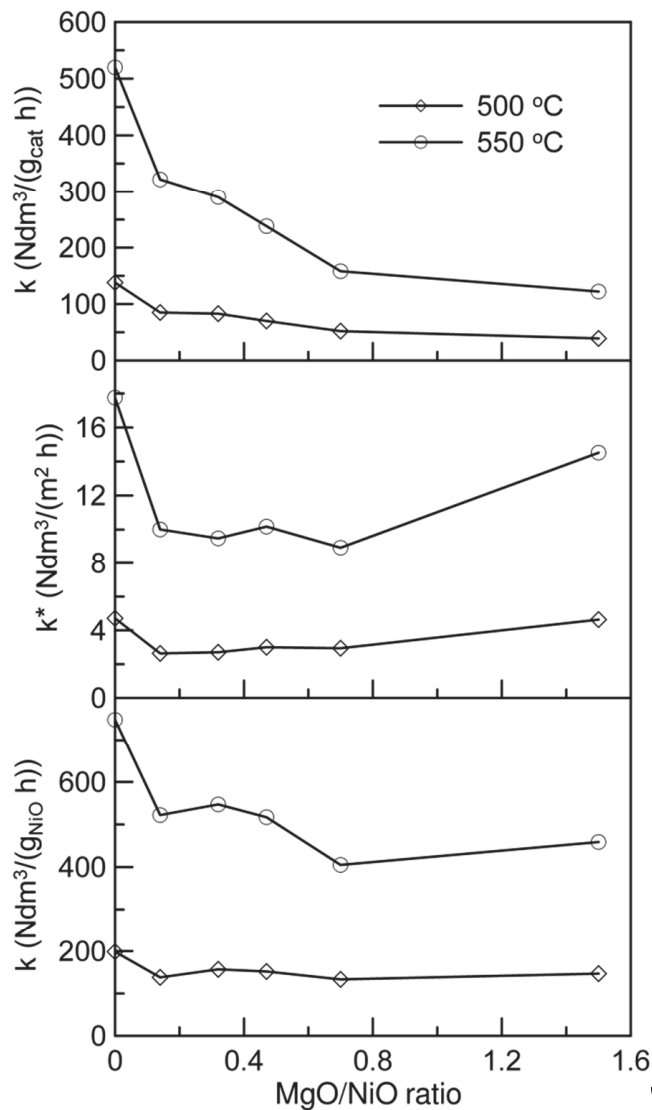


Fig. 3. The rate constants per unit of the catalyst weight, unit of the active surface area and unit of the NiO content determined at the constant $\text{H}_2\text{O}:\text{CH}_4 = 2$ ratio.

In this way we can exclude the effect of the $\text{H}_2\text{O}:\text{CH}_4$ ratio on the rate constants values. The activity of 1 g of the catalysts gradually decreases as the MgO/NiO ratio increases. The specific activity (per unit of the active surface area) initially decreases for the catalyst B1 (MgO/NiO ratio = 0.14) and then it remains at almost constant level until the MgO/NiO ratio reaches 0.7. Further increase of the MgO/NiO ratio to 1.5 leads to some increase of the activity though it does not reach the value corresponding to the B0 catalyst. Figure 3 also shows that the rate constants per unit of the NiO content in a catalyst decreases slightly with the increase the MgO/NiO ratio.

It becomes evident that, the increasing amount of MgO reduces the rate constants though its influence is not that strong.

From the Arrhenius plots the activation energies and pre-exponential factors were calculated using the rate constants determined for the constant amount of hydrogen (~4 vol.%) in the reagents mixture and similar H₂O:CH₄ ratios. As shown in Fig. 4 the activation energies vary from 111 to 123 kJ/mol. The observed higher activities of B0 and B5 catalysts result from higher values of the pre-exponential factors as the activation energies are almost the same in every case.

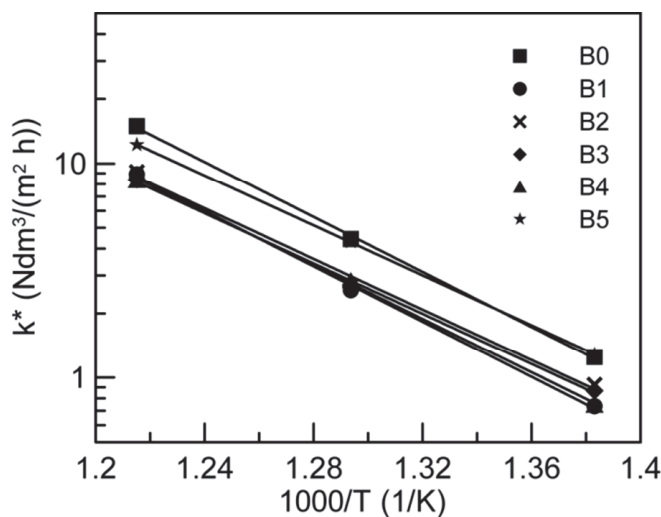


Fig. 4. The temperature dependence of the catalysts activity calculated per unit of the active surface area.

3.4. Coking

3.4.1. Coking in the steam reforming of methane

Studies of the catalysts coking are an important part of the catalytic tests. This is because the catalysts exhibiting high initial activity are easier to be obtained than catalysts with long-term resistance to deactivation. Many catalytic reactions involving hydrocarbons or carbon oxides are accompanied by the coking phenomenon. Its origin is related to the interaction of reagents (or gasifying factors such as steam, carbon dioxide, oxygen or hydrogen also) with the catalysts surface [7, 32, 33].

Preliminary studies by the TPSR method have shown that at the reagents ratio H₂O:CH₄ = 0.8 only the B0 catalyst has exhibited the carbon deposit formation and this process started to occur only at a high temperature, i.e. 827°C. The other samples were totally resistant to the

coke formation even at the temperatures of about 850°C. Further studies were carried out at the reagents ratio $\text{H}_2\text{O}:\text{CH}_4 = 0.3$. The temperatures of the coking initiation differ insignificantly from each other and cover the range from 612 to 621°C. Figure 5 shows that the highest temperature of the coking initiation and the temperature corresponding to the deposition of 10 wt.% of coke (when referred to the initial catalysts weight) was observed for the catalyst B4 (the ratio $\text{MgO}/\text{NiO} = 0.7$). This catalyst is, thus, the most resistant to deactivation via coke formation during the reaction.

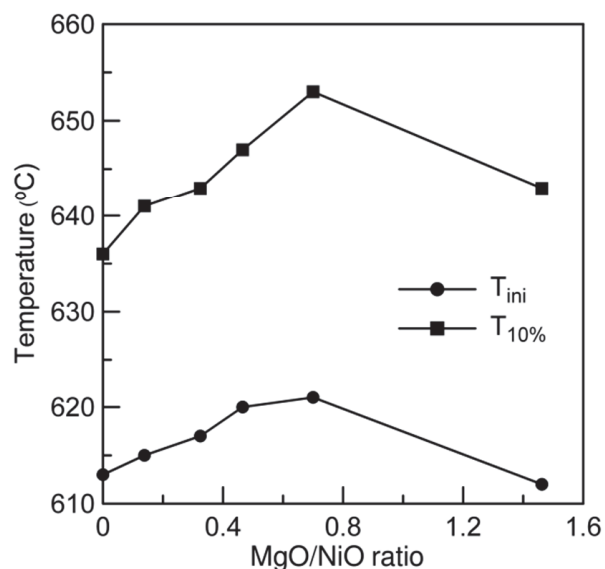


Fig. 5. The temperatures of the coking initiation and temperatures corresponding to the deposition of 10 wt.% of coke as a function of the MgO/NiO ratio in the steam reforming of methane.

3.4.2. Coking in the steam reforming of n-butane

The coking process in the TPSR method is a function of two variables: temperature and time. In view of small differences between the temperatures of the coking initiation in the steam reforming of methane, it is reasonable to verify these results using higher hydrocarbons, i.e. *n*-butane, which normally enhances the coking phenomena [19, 32] and to apply the isothermal gravimetric method.

Isothermal measurements allow for a continuous monitoring of the deposit amount formed. Initially, a non-linear and slow increase of the sample weight is observed and the duration of this initial stage may be various depending on the reaction conditions and the catalyst. Afterwards, the sample weight increases linearly with time and in the literature this

stage is called the *steady-state rate of deposition* [33-35]. The rate of coking, determined from the linear sections of the weight vs time curves, and referred to either the catalyst unit weight or unit of the active surface area, is normally used for comparison of the coking resistance of the samples. These studies were carried out at the temperature of ca. 500°C, which corresponds to the maximum of the coking rate in the reforming of higher hydrocarbons [8, 37]. Figure 6 shows how the amounts of carbon deposits increase with the reaction time in the steam reforming of *n*-butane at the reagents ratio $\text{H}_2\text{O}:\text{C} = 0.5$.

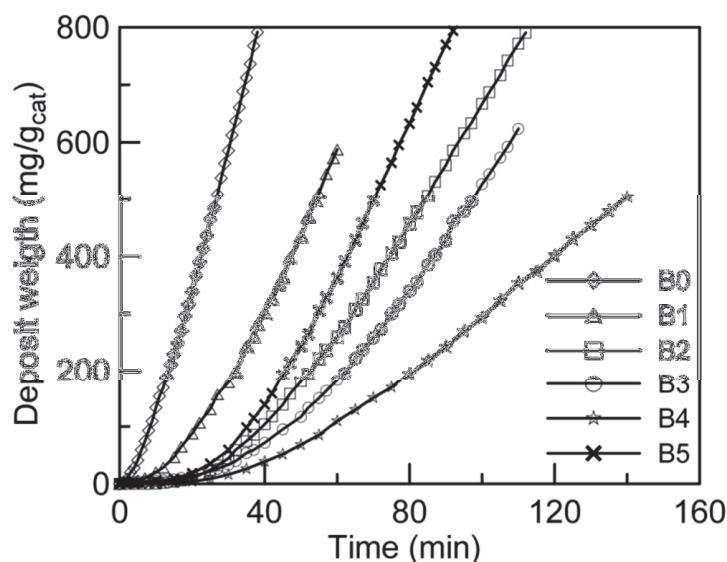


Fig. 6. Carbon deposit weight vs time in the steam reforming of *n*-butane. ($T = 500^\circ\text{C}$, $\text{H}_2\text{O}:\text{C} = 0.5$)

The coking rates, r_C , determined from the slopes of the linear sections, indicate that there is some optimal amount of MgO (21.4–27.3 wt.%), for which the catalysts reveal the highest resistance to coking. Further increase of the MgO content leads again to the increase of the coking rate. The second important parameter describing the resistance to coking is the so-called induction time. It can be determined from the deposit weight vs time curves as the time at which the enlarged linear section of the curve crosses the time axis [33, 36]. For highly resistant catalysts the induction times might reach large values [38, 39].

Figure 7 shows the determined induction times as well as the coking rates (at 10 wt.% of the initial catalyst weight of the deposit formed) as functions of the MgO/NiO ratio in the steam reforming of *n*-butane.

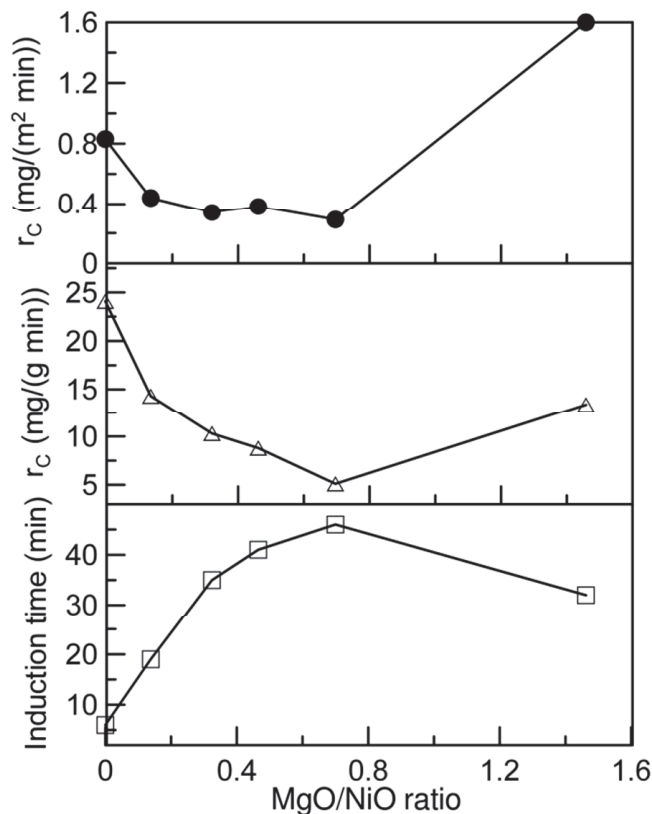


Fig. 7. Coking parameters in the steam reforming of *n*-butane as a function of the MgO/NiO ratio ($T = 500^\circ\text{C}$, $\text{H}_2\text{O}:\text{C} = 0.5$); (r_c – determined at 10 wt.% of the initial catalysts weight of the deposit formed).

The results indicate that in both reforming reaction of methane or *n*-butane, a maximum of the coking resistance exists for the catalyst B4 with the MgO/NiO ratio of ca. 0.7. This catalyst exhibits the highest temperature of the coking initiation in the case of the methane reforming and the longest induction time and the smallest coking rate in the case of the *n*-butane reforming.

In order to estimate an influence of the reagents ratio on the coking rate, similar studies were carried out using the higher $\text{H}_2\text{O}:\text{C}_4\text{H}_{10}$ ratio, corresponding to $\text{H}_2\text{O}:\text{C} = 1.5$. Only the nickel catalyst B0 has exhibited some small coke production within the considered period of several hours (results not shown).

3.4. The properties of the carbon deposits

Significant differences in the coking process for various catalysts raise the question about the influence of the catalyst composition

(MgO/NiO ratio) on the nature and properties of the carbon deposits formed.

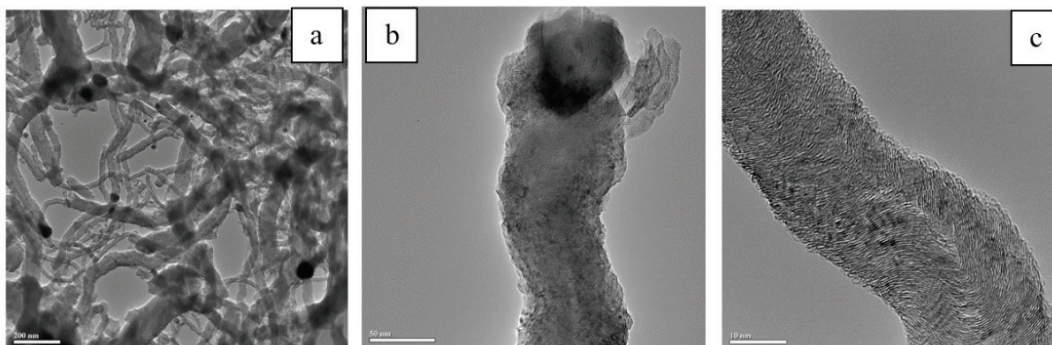


Fig. 8. Carbon deposits on B0 catalyst.

The morphology of fibrous deposits formed on the studied catalysts in *n*-butane steam reforming (Fig. 8) was typical for this reaction [17, 38, 40] and its low temperature [17, 41]. A typical fiber is made of poorly ordered carbon (although there is some ordering of the graphite layers – Fig. 8c). In the middle of the fibers there is a narrow channel (empty or filled with amorphous carbon). The fibers are terminated with a nickel metal particle (Fig. 8b).

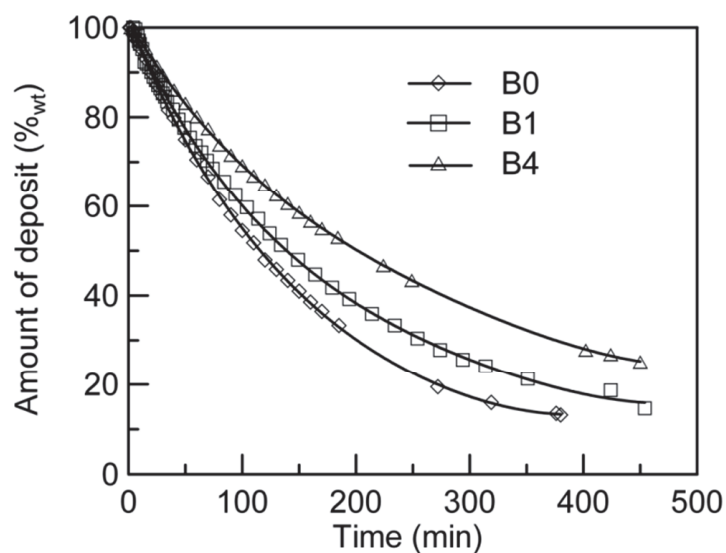


Fig. 9. Isothermal (500°C) hydrogenation of carbon deposits produced during the steam reforming of *n*-butane at the reagents ratio $H_2O:C=0.5$.

The deposits produced during the steam reforming of *n*-butane were gasified according to two approaches: using the isothermal gravimetric

method with hydrogen as the gasifying agent and using the temperature-programmed oxidation (TPO). Figure 9 shows the isothermal decoking curves for the selected catalysts at the temperature of 500°C.

The carbon deposit removal proceeds with various rates depending on the catalyst composition. The rates of the catalyst weight uptakes follow the same trend as the coking rates (Fig. 6), i.e. B0 > B1 > B4.

Figure 10 shows the TPO curves determined for the catalysts coked. As it can be seen, the catalyst composition has almost no effect on the temperature of the gasification maximum rate (~610°C).

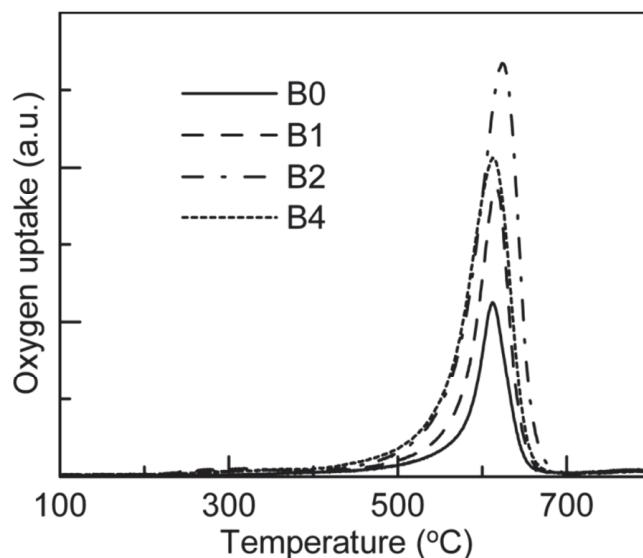


Fig. 10. The TPO curves determined for the catalysts coked in the steam reforming of *n*-butane.

4. DISSCUSION

The modification of the catalyst composition (the MgO:NiO ratio) leads to changes of the nickel state due to influence on the NiO reduction degree, development of the nickel surface area and its dispersion. The state of the active phase affects the most important properties of the studied catalysts: activities and resistance to coking.

The introduction of magnesia into the catalysts leads to changes in the surface properties of nickel crystallites. Studies of the temperature-programmed desorption of hydrogen give, normally, an insight into the nature or quantity of the active centers on the catalyst surface. The TPD-H₂ profiles of catalysts with the variable MgO/NiO ratios were

subjected to a quantitative analysis in ref. [42]. The determined adsorption energy distribution functions showed that the catalysts containing ≤ 27.3 wt.% of MgO revealed qualitatively similar bands of the adsorption energy. Only the catalyst containing 38.9 wt.% of MgO differs substantially from the others. However, the increasing amount of MgO alters the population of various types of adsorption centers found on catalysts active phases. Thus, the amount of MgO modifies significantly the morphology of nickel crystallites formed during the reduction process [42].

In the steam reforming of methane (Fig. 3) a relatively broad minimum of the specific activity was found in the range of MgO:NiO ratios from 0.14 to 0.7. In the same range the catalysts studied exhibit the smallest mean sizes of nickel crystallites (d_x).

As it is shown in Fig. 11 the specific activity increases linearly with the mean nickel crystallites size. This suggests the existence of the structure sensitivity [43-45] of the methane steam reforming reaction.

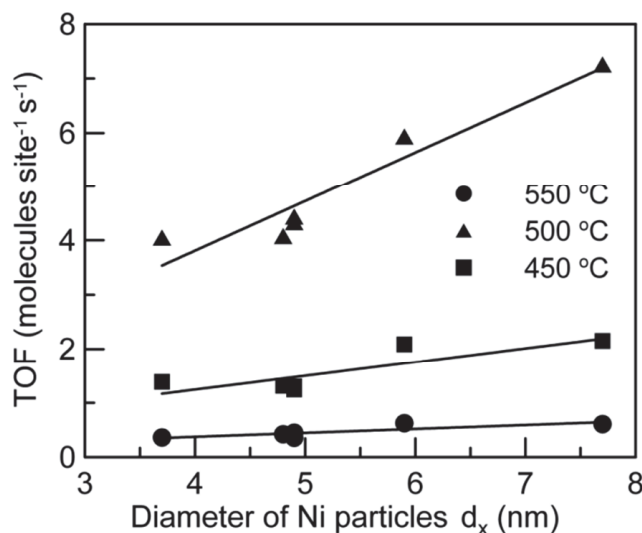


Fig. 11. Influence of the mean nickel crystallites sizes on the activity of catalysts in the steam reforming of methane.

The phenomenon of the structure sensitivity in steam reforming has not been reported very often in the literature so far. Parmaliana *et al.* [46] have found the existence of the maximum activity of the Ni/MgO catalysts in the range of nickel crystallites from 9 to 13 nm. Within the range from 2 to 9 nm the activity increased, whereas from 9 to 13 nm a decreasing trend has been observed. The increase of the activity for mean sizes of nickel

crystallites in the range 3.7–8 nm (Fig. 11) confirms the results found in literature [46].

Other results have been published in [47, 48]. Jones *et al.* [47] have shown for some metals, including Ni, that the reaction rate of the steam reforming of methane at the temperature 500°C increases with the increasing dispersion up to $D = 40\%$. However, it should be emphasized, that in [47] there are no source data concerning the discussed relationship as well as a detailed information about the catalysts. In the CO₂ reforming of methane Wang *et al.* [48] have found the decrease of activity with the increasing size of crystallites for Ni/MgO catalysts with various contents of Ni (3.4–45 wt.%) and various calcination temperatures (400–950°C). However, some doubts arise concerning the methods used to calculate the nickel dispersion based on the data from TPD-H₂ and TPR measurements, particularly for the samples with the highest dispersion ($d_{Ni} \leq 4.5\text{nm}$) calcined at highest temperatures ($> 650^\circ\text{C}$). Under such conditions the degree of NiO reduction was lower than 14%, thus the error concerning hydrogen uptake could be the largest. Therefore, it seems that the question about the structure sensitivity of the steam reforming reaction has not been answered and this issue requires further studies.

The modifications of the catalysts composition (the MgO:NiO ratio) affect significantly the resistance to coking either in the steam reforming of methane or *n*-butane (Figs. 5 and 7, respectively). The catalysts with the MgO:NiO ratio ranging from 0.14 to 0.7 exhibit promising properties (enhanced resistance to the coke formation). This is clearly illustrated in the studies of the steam reforming of *n*-butane. Even a small addition of MgO (~10 wt.%) to the NiO–Al₂O₃ system leads to a substantial decrease of the coking rate, r_C and it levels off until the MgO:NiO ratio reaches 0.7. Further increase of that ratio enhances the coking rate (Fig. 7). The most resistant to coking, in both reactions, is thus the catalyst containing 27.3 wt.% of MgO.

The resistance to coking is affected by the presence of the acid centers on the catalysts surfaces [15, 20, 49-51]. For the studied catalysts in [11] it has been shown, that the acid centers density decrease with the increasing MgO:NiO ratio in the range from 0.14 to 0.7, with a minimum for the ratio ~0.3. However, decreasing of the surface acidity cannot be the only reason for changes in the coking rate.

The coking rate, r_C as a function of the catalyst composition correlates well with the mean size of nickel crystallites. The catalyst with the MgO/NiO ratio equal to 0.7 reveals the lowest coking rate and the longest induction time of coking (Fig. 8), at the same time it shows the highest dispersion of nickel. Figure 12 underlines the linear relationship

between the coking rate and the mean size of nickel crystallites. The increase of the nickel dispersion leads to the decrease of the coking rate. This relationship confirms again a strong influence of the nickel dispersion on the course of processes leading to the coke formation, reported in literature [2,52-55].

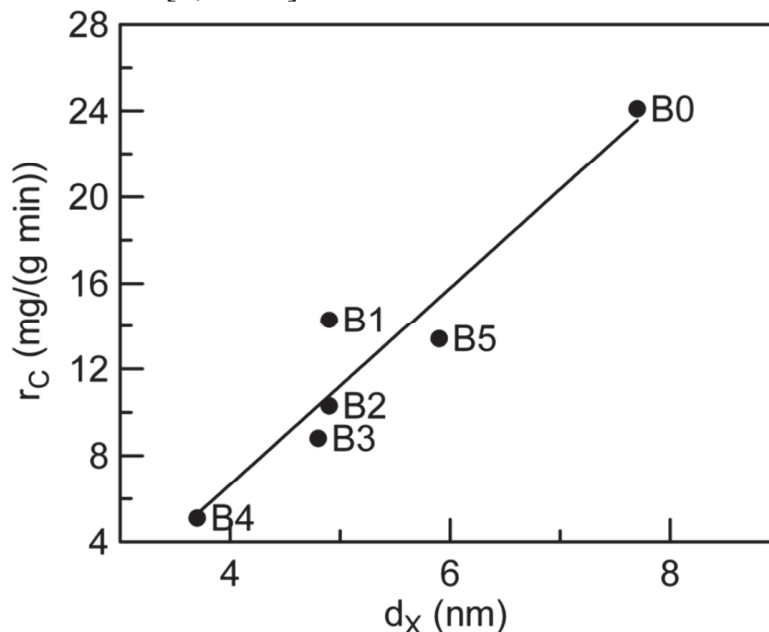


Fig. 12. The coking rate as a function of the mean sizes of nickel crystallites for the catalysts studied.

The apparent inconsistency observed in the results of the carbon deposits gasification using both isothermal and temperature-programmed oxidation methods; can be explained by taking into account the mechanisms of their formation.

In the steam reforming of hydrocarbons the main type of carbon deposits are the so-called *filamentous deposits* [15,19,38,41,56]. The nickel crystallites are placed on the top of filaments and, during the reaction, they are lifted by the developing carbon filaments [19,38,56-60]. The processes occurring on the nickel crystallites affect coking as well as decoking processes. A lower coking rate indicates that some portion of nickel crystallites does not take part in coke formation processes because of e.g. small sizes [2,52-55] or surface composition [61-63]. The „in situ” observations using the SEM technique showed that the coke formation processes and coke gasification were reversible and proceeded according to the same mechanism [64].

The studied deposits are the same (Fig. 10). Thus, the differences in the coking rates are not related to the changes of the deposits properties but to smaller amounts of the coked crystallites. However, although the total removal of the deposits is possible, it does not result in the full regeneration of the catalysts because their initial state cannot anyway be recovered [65, 66].

As it can be concluded from our studies the crucial factor controlling the properties of composite Ni/MgO–Al₂O₃ catalysts is the nickel dispersion which, in turn, depends on the catalyst composition and its initial treatment.

The existence of a wide range of the MgO to NiO ratios, for which the catalysts exhibit a high resistance to coking is very promising. It should facilitate the optimization of other properties, including the activity, without a negative influence on the resistance to coking.

Table 3 compares the coking parameters of the catalysts studied in the steam reforming of hydrocarbons. The shaded areas underline the catalyst composition providing the highest resistance to coking in a given reaction.

Table 3. The coking parameters of the catalysts studied.

Coking parameter	MgO/NiO ratio					
	0	0.14	0.32	0.47	0.7	1.5
C ₄ H ₁₀ + H ₂ O [H ₂ O:C = 0.5] Induction time [min]	6	20	35	41	46	32
CH ₄ + H ₂ O [H ₂ O:C = 0.3] Temperature of the coking initiation [°C]	613	615	616	620	621	612

5. CONCLUSIONS

The NiO–MgO–Al₂O₃ catalysts were investigated in order to find the optimal composition in terms of the activity and resistance to coking. It was found that all the catalysts containing MgO exhibited a higher reduction temperature than the standard alumina-supported nickel

catalysts. The increasing amounts of the MgO lead to a gradual decrease of the reduction degree and increase of the maximum of the TPR peaks. It means that the presence of MgO facilitates the formation of hardly reducible compounds containing NiO such as NiO–MgO solid solutions or MgAl₂O₄ spinel.

The activity of catalysts depends on the composition though its value only slightly depends on the amount of MgO. The highest activity was observed for the catalysts without MgO; a small addition of MgO reduced the activity to some extent but it remained at almost constant level as the amount of MgO increased. Furthermore, it was found a correlation between the mean size of nickel crystallites and the catalysts activity. Within the size range from 3.7 to 8.0 nm the activity increases linearly what suggests the existence of the structure sensitivity of the reaction.

The presence of MgO reduces the coke formation in the steam reforming of methane and *n*-butane. The coking rate was found to decrease with the increasing dispersion of nickel crystallites. The highest resistance to coking was observed for the catalyst containing 27.3 wt.% MgO, which, revealed also the highest dispersion of nickel crystallites. The properties of carbon deposits turned out to be of the same type (the same temperature of the maximum for the TPO peaks), though the rates of coking and decoking depended on the catalysts composition.

Thus, the nickel crystallites sizes turn out to be a very important parameter affecting either the activity or resistance to the coke formation. It seems that this parameter directly affects the catalysts properties. Other parameters like the amount of MgO, preparation technique, calcination conditions and the reduction degree of NiO affect the catalysts properties indirectly through modification of the nickel crystallites morphology.

6. ACKNOWLEDGEMENTS

The research was carried out with the financial support of statutory funds for R&D activities. The authors thank dr W. Gac for carrying out TPO research.

REFERENCES

- [1] E. Ruckenstein, Y-H. Hu, *Appl. Catal. A:Gen.*, **133**, 149, (1995).
- [2] T. Borowiecki, *Appl. Catal.*, **31**, 207, (1987).

- [3] Y-H. Hu, E. Ruckenstein, *Catal. Rev. - Sci. Eng.*, **44**, 423, (2002).
- [4] F. Melo, N. Morlanes, *Catal. Today*, **107-108**, 458, (2005).
- [5] F. Melo, N. Morlanes, *Catal. Today*, **133**, 374, (2008).
- [6] F. Melo, N. Morlanes, *Catal. Today*, **133**, 383, (2008).
- [7] M.T. Fan, K.P. Miao, J.D. Lin, H.B. Zhang, D.W. Liao, *Appl. Surf. Sci.*, **307**, 682, (2014).
- [8] T. Borowiecki, *Appl. Catal.*, **10**, 273, (1984).
- [9] F. Arena, B.A. Horrell, D.L. Cocke, A. Parmaliana, N. Giordano, *J. Catal.*, **132**, 58, (1991).
- [10] K.Y. Koo, M.G. Park, U.H. Jung, S.H. Kim, W.L. Yoon, *Int. J. Hydrogen Energy*, **39**, 10941, (2014).
- [11] W. Gac, *Appl. Surf. Sci.* **257**, 2875, (2011).
- [12] D.R. Ridler, M.V. Twigg, in: *Catalyst Handbook*, 2nd ed., (M.V. Twigg, Ed.), Wolfe Publishing Ltd.: London, p. 225, (1989)
- [13] K. Tomishige, Y-G. Chen, K.J. Fujimoto, *J. Catal.*, **181**, 91, (1999).
- [14] Z. Alipour, M. Rezaei, F. Mashkani, *J. Ind. Eng. Chem.*, **20**, 2858, (2014).
- [15] M.A. Nieva, M.M. Villaverde, A. Monzon, R.T.F. Garetto, A.J. Marchi, *Chem. Eng. J.*, **235**, 158, (2014).
- [16] S.D. Angeli, F.G. Pilitsis, A.A. Lemonidou, *Catal. Today*, **242**, 119, (2015).
- [17] J.R. Rostrup-Nielsen, in: *Catalysis - Science and Technology*, (A.R. Anderson, M. Boudart, Eds.), Vol. 5, Springer Verlag, Berlin, p. 1, 1984
- [18] J.R. Rostrup-Nielsen, *J. Catal.*, **31**, 173, (1973).
- [19] J.R. Rostrup-Nielsen, B.P. Tottrup, in: *Symposium on Science of Catalysis and its Application in Industry*, FPDIL, Sindri, India, February 22-24, Paper No. 39, p. 379, (1979).
- [20] I. Alstrup, B.S. Clausen, C. Olsen, R.H.H. Smits, J.R. Rostrup-Nielsen, in: *Natural Gas Conversion V*, (Parmaliana A. et al.: Eds.), Stud.Surf.Sci.Catal, Vol. 119, Elsevier, Amsterdam, p. 5, (1998)
- [21] K.Y. Koo, H-S. Roh, Y.T. Seo, D.J. Seo, W.L. Yoon, S.B. Park, *Appl. Catal. A: Gen.*, **340**, 183, (2008).
- [22] C.H. Bartholomew, R.J. Farrauto, *J. Catal.*, **45**, 41, (1975).
- [23] G. Bergeret, P. Gallezot, in: *Handbook of Heterogeneous Catalysis*, (G. Ertl, H. Knozinger, J. Weitkamp, Eds.), Vol. 2, VCH Verlag, Weinheim, p. 439, (1997)
- [24] J. Zieliński, *React. Kinet. Catal. Lett.*, **17**, 69, (1981).
- [25] T. Borowiecki, W. Grzegorzczak, A. Denis, A. Gołębiowski, *Catal. Lett.*, **79**, 119, (2002).
- [26] T. Borowiecki, W. Grzegorzczak, A. Denis, A. Gołębiowski, *React. Kinet. Catal. Lett.*, **77**, 163, (2002).
- [27] W. Gac, A. Denis, T. Borowiecki, L. Kępiński, *Appl. Catal. A: Gen.*, **357**, 236, (2009).
- [28] A. Parmaliana, F. Arena, F. Frusteri, N. Giordano, *J. Chem. Soc. Farad. Trans.*, **86**, 2663, (1990).

- [29] B. Scheffer, P. Molhoek, J.A. Moulijn, *Appl. Catal.*, **46**, 11, (1989).
- [30] F. Arena, A. Parmaliana, N. Mondello, F. Frusteri, N. Giordano, *Langmuir*, **7**, 1555, (1991).
- [31] J.T. Richardson, B. Turk, M.V. Twigg, *Appl. Catal. A: Gen.*, **148**, 97, (1996).
- [32] D.L. Trimm, *Catal. Today*, **37**, 233, (1997).
- [33] J.R. Rostrup-Nielsen, *Steam Reforming Catalysts*, Teknisk Forlag A/S, Copenhagen, (1975)
- [34] Q. Zhuang, Y. Qin, L. Chang, *Appl. Catal.*, **70**, 1, (1991).
- [35] D.C. Gardner, C.H. Bartholomew, *I&EC Prod. Res. Dev.*, **20**, 80, (1981).
- [36] T. Borowiecki, A. Machocki, J. Ryczkowski, in: *Catalyst Deactivation 1994*, (B. Delmon, G.F. Froment, Eds.) Vol. 88, Stud.Surf.Sci.Catal., Elsevier, Amsterdam, p. 537, (1994)
- [37] T. Borowiecki, *Polish J. Chem.*, **67**, 1755, (1993).
- [38] J.W. Snoeck, G.F. Froment, M. Fowles, *J. Catal.*, **169**, 240, (1997).
- [39] T. Borowiecki, A. Machocki, in: *Catalyst Deactivation 1999*, (B. Delmon, G.F. Froment Eds.), Vol. 126, Stud.Surf.Sci.Catal., Elsevier, Amsterdam, p. 435. (1999).
- [40] C.H. Bartholomew, *Catal.Rev.-Sci.Eng.*, **24**, 67-112, (1982).
- [41] E. Tracz, R. Scholtz, T. Borowiecki, *Appl. Catal.*, **66**, 133, (1990).
- [42] T. Pańczyk, W. Gac, M. Pańczyk, A. Dominko, T. Borowiecki, W. Rudzinski, *Langmuir*, **21**, 7311, (2005).
- [43] M. Boudart, in: *Adv. Catal.*, (D.D. Eley, H. Pines, B.D. Weisz, Eds.), Vol. 20, Elsevier, Amsterdam, p. 153, 1969
- [44] M. Che, C.O. Bennett, in: *Adv. Catal.*, (D.D. Eley, H. Pines, B.D. Weisz, Eds.), Vol. 36, Elsevier, Amsterdam, p. 55, 1989
- [45] V. Ponec, G.C. Bond, in: *Stud.Surf.Sci.Catal*, Vol. 95, Elsevier, Amsterdam, p. 280, 1995
- [46] A. Parmaliana, F. Arena, F. Frusteri, S. Coluccia, L. Marchera, G. Martra, L. Chuvilin, *J. Catal.*, **141**, 34, (1993).
- [47] G. Jones, J.G. Jakobsen, S.S. Shim, J. Kleis, M.P. Andersson, J. Rossmesl, F. Abild-Pedersen, T. Bligaard, S. Helveg, B. Hinnemann, J.R. Rostrup-Nielsen, Ib. Chorkendorff, J. Sehested, J.K. Nørskov, *J. Catal.*, **259**, 147, (2008).
- [48] Y-H. Wang, H-M. Liu, B-Q. Xu, *J. Molec. Catal. A:Gen.*, **299**, 44, (2009).
- [49] S.P.S. Andrew, *Ind. &EC Prod. Res. Dev.*, **8**, 321, (1969).
- [50] T. Borowiecki, A. Denis, W. Gac, M. Pańczyk, B. Stasińska, in: *Heterogeneous Catalysis, Proc. 9th Intern. Symp.*, Bułgaria, Varna 2000, (L. Petrov, Ch. Bonev, G. Kadinov, Eds.), Institute of Catalysis, Bul. Academy of Sciences, Bułgaria, p. 913, 2000
- [51] A. Gołębiowski, K. Stołeczki, U. Prokop, A. Kuśmierowska, T. Borowiecki, A. Denis, Cz. Sikorska, *React. Kinet. Catal. Lett.*, **82**, 179, (2004).
- [52] J.R. Rostrup-Nielsen, *J. Catal.*, **85**, 31, (1984).

- [53] T. Borowiecki, *Appl. Catal.*, **4**, 223, (1982).
- [54] D. Duprez, A. Miloudi, J. Little, J. Bousquet, *Appl. Catal.*, **5**, 219, (1983).
- [55] H.S. Bengaard, J.K. Norskov, J. Sehested, B.S. Clausen, L.P. Nielsen, A.M. Molenbroek, J.R. Rostrup-Nielsen, *J. Catal.*, **209**, 365, (2002).
- [56] L. Kępiński, B. Stasińska, T. Borowiecki, *Carbon*, **38**, 1845, (2000).
- [57] J.R. Rostrup-Nielsen, D.L. Trimm, *J. Catal.*, **48**, 155, (1977).
- [58] D.L. Trimm, *Catal. Rev.-Sci. Eng.*, **16**, 155, (1997).
- [59] R.T.K. Baker, *Catal. Rev. Sci. Eng.*, **19**, 161, (1979).
- [60] I. Alstrup, *J. Catal.*, **109**, 241, (1988).
- [61] T. Borowiecki, A. Denis, W. Gac, R. Dziembaj, M. Drozdek, Z. Piwowarska, *Appl. Catal. A: Gen.*, **274**, 259, (2004).
- [62] J.R. Rostrup-Nielsen, J. Sehested, J.K. Norskov, in: *Adv. Catal.*, (B.C. Gates, H. Knozinger, Eds.), Vol. 47, Elsevier, Amsterdam, p. 65, 2002
- [63] B. Stasińska, J. Gryglicki, T. Borowiecki, in: *Heterogeneous Catalysis, Proc.8th Int. Symp. Heterogeneous Catalysis, Bulgaria, Varna, 5-9 October 1996*, (A. Andreev et al. Eds.), Institute of Catalysis, Bul. Academy of Sciences, Bułgaria, Sofia, p. 879, 1996
- [64] J.L. Figueiredo, C.A. Bernardo, J.J. Chludziński, R.T. Baker, *J. Catal.*, **110**, 127, (1988).
- [65] J.L. Figueiredo, D.L. Trimm, *J. Catal.*, **40**, 154,
- [66] J.L. Figueiredo, *Carbon*, **19**, 146, (1981).